Chapter 7

Soft Sediment Deformation Structures Triggered by the Earthquakes: Response to the High Frequent Tectonic Events during the Main Tectonic Movements

Bizhu He, Xiufu Qiao, Haibing Li and Dechen Su

Additional information is available at the end of the chapter

http://dx.doi.org/10.5772/intechopen.72941

Abstract

Typical cases of the soft-sediment deformation structures (SSDSs), triggered by the modern earthquakes to the oldest of paleo-earthquakes in the Mesoproterozoic, have been observed in China. These deformation structures have various geometry morphology, different interior structural architectures and sediment compositions, in centimetre to metre-scales. They are intercalated with the undeformed layers, which are composed of similar sediments of lithology and sedimentary environments. SSDSs are formed during sediments deposited but incompletely consolidated. And they exist in different periods and are closely related to the active or paleo-active faults. They occur nearby the faults and usually have the characteristics nearer to the faults and more. And they distribute parallel to the trending of the active faults and have the characters of the vertical duplication. They have responded to the high-frequency activity of different faults in tectonic movement and are the perfect records of the paleo-active faults.

Keywords: soft sediment deformation structure, triggering mechanism, records of earthquakes, high-frequent tectonic events, paleo-active faults

1. Introduction

Under regional tectonic stress, the earth's interior might become imbalanced and the stored elastic strain energy inside the earth would be released quickly, and so the seismic events occur and cause devastating disasters to the life and environment [1–3]. Earthquakes are derived from plate tectonic movements [4–6]. Earthquakes occur primarily at the boundaries between lithospheric plates, such as divergence zone, transform zone and convergence zone,

and also occur at the pre-existing fault or weak stress belt in the plate and can be triggered by impacting of meteorites [7].

Paleo-seismic records are induced by earthquakes during geological history and reserved in strata. They include two categories: fault rocks and seismites. The fault rocks are composed of cataclastic rocks, mylonites, pseudotachylytes and fault gouge. They can occur and have been preserved at active fault zones and their adjacent areas in different geological times. The fault rocks are formed in different focal mechanisms of normal faults, thrust faults and strike slip faults [8–12, 5, 13]. Pseudotachylytes can be thought of as "an earthquake fossil". The fault rocks can be as the records of the active fault during different times. But the fault zone is often located in the long-term tectonic activity areas, and the later tectonic activities are often superimposed on the previous activities. Therefore, it is difficult to distinguish them for different time and determine the activity of faults.

Seismites are the soft-sediment deformation structures (SSDSs) produced by strong earthquakes. SSDS is deformation that originates in unconsolidated sediments and usually occurs rapidly at or close to the surface during or shortly after deposition and before lithification takes place. During the deformation process, the original sediment particles are rearranged and migrated, the compositions are not changed and no new minerals would be produced. The triggers for SSDS are tectonism, glaciogenic, mass movement, collapse and some other physical and biological processes, and the earthquake trigger is one of important dynamic drives. Seismites had been observed from 1780s [14], and the liquefaction triggered by modern earthquakes were mainly studied. But the term 'seismites' was first proposed by A. Seilacher to interpret an effect of strong earthquakes on paleoslope for fault-graded beds in the Monterey Shales (Miocene), the north of Santa Barbara, California (USA) [15]. From the 1970s to 2000, several SSDSs triggered by earthquakes were identified and the formation mechanisms were primarily analysed [16–18]. In the last 20 years, they have been widely developed and classified [14, 19–21]. The special SSDSs (seismites) with inconsistence are preserved in the normal sedimentary strata, which provide opportunities to understand tectonic activity at different times.

In this chapter, we introduce the typical SSDSs observed in China, which are triggered by the recent to the Mesoproterozoic earthquake activities, and formed in different deposition environments and are composed of different sedimentary rocks. Especially, the structural styles, preserved positions, occurrence times, formation mechanisms and relationship with the activities of faults are discussed. The aim of the chapter is to reveal the high-frequency active events of the faults in different geological history and provide evidences for the paleotectonic and paleogeographic reconstruction.

2. Genetic mechanisms of soft-sediment deformation structures

Soft-sediment deformation structures (SSDSs) are deformations that originated in unconsolidated sediments [16, 18, 19]. SSDSs can occur in different tectonic settings, e.g., passive continental margins, deep (trench) subduction zones and strike-slip tectonic transitions,

and they can form in almost all sedimentary environments, preferably in shallow-marine, lagoonal, lacustrine and fluvial environments.

There are mainly four deformation mechanisms: (1) intergranular shear [22, 23]; (2) plastic or hydroplastics [24, 25]; (3) liquefaction [18, 24, 27] and (4) fluidization [24, 26]. The driving forces of deformation mechanisms include the tectonism, gravity acting on slopes, disequilibrium loading caused by topographical irregularities in the sediment-water interface, gravitational instabilities due to a reverse density gradient where denser sediments overlie less dense sediments, shear waves or other currents, and biological and chemical agents [14, 15, 18, 27–29]. The various morphology and deformation styles of the SSDSs can be formed with respect to sedimentation in different lithology, driving forces, sediment rheology and deformation mechanisms of the deformation [20, 27, 30–33].

Numerous schemes of classification of SSDSs have been proposed [14, 24, 26, 28, 29, 32]. The formation mechanisms of deformations induced in earthquake may be classified into five main categories, which include liquefaction, thixotropic deformation, hydroplastication, superposed gravity driving deformation and brittle deformation. And the secondary classification is also proposed according to genetic types, sediment compositions and deformation styles (**Figure 1**).

The strict criteria of SSDSs triggered by seismic events (seismites) have been discussed [14, 15, 18, 20, 27, 28, 34]. The commonly received criteria include (1) the deformation emerges in laterally continuous, vertically recurring layers, separated by undeformed layers; (2) the deformation occurs in marine, lacustrine or fluvial sediments; (3) deformed and undeformed beds have similar lithologies and facies features; (4) the deformation is related to a seismically or tectonically active area; (5) the deformation shows systematic increases in frequency or intensity toward a likely epicentral area. "Liquefied deformation" as a seismic record is associated with many modern and ancient seismogenic deposits and is related to surface-wave magnitudes Ms > 5 [20, 30, 32, 35].

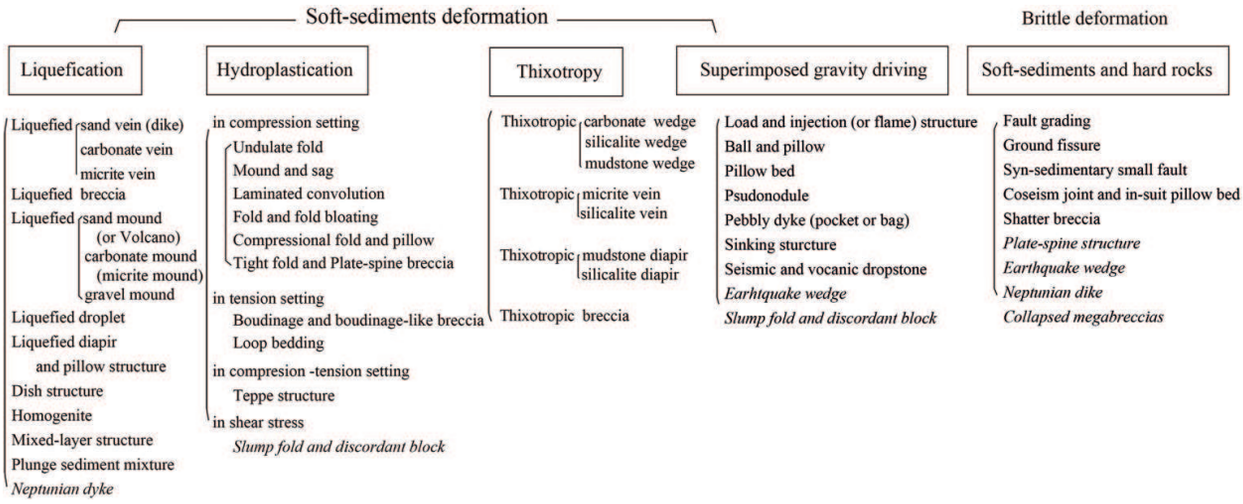

Figure 1. Classification of SSDSs according to the genetic mechanism (modified from [14, 18, 20, 21]). The deformations in italics are triggered by more than two mechanisms.

3. Typical cases of the SSDSs triggered by earthquakes during the geological history

3.1. Triggered by the modern earthquakes of the Yingxiu-Beichuan active faults

The MS 8.0 Wenchuan earthquake struck the Longmenshan area on 12 May 2008, the transition zone between the eastern margin of the Tibetan Plateau and the Sichuan Basin, China. Besides the huge casualties and property losses, a most complicated yet longest thrust-type co-seismic surface rupture zone was developed in the quake-hit area. The surface rupture extends over lengths of 270 km and 80 km along the NE-SW trending Yingxiu-Beichuan fault (hereafter YBF) and Guanxian-Anxian fault (hereafter GAF) (**Figure 2**), which are high-angle

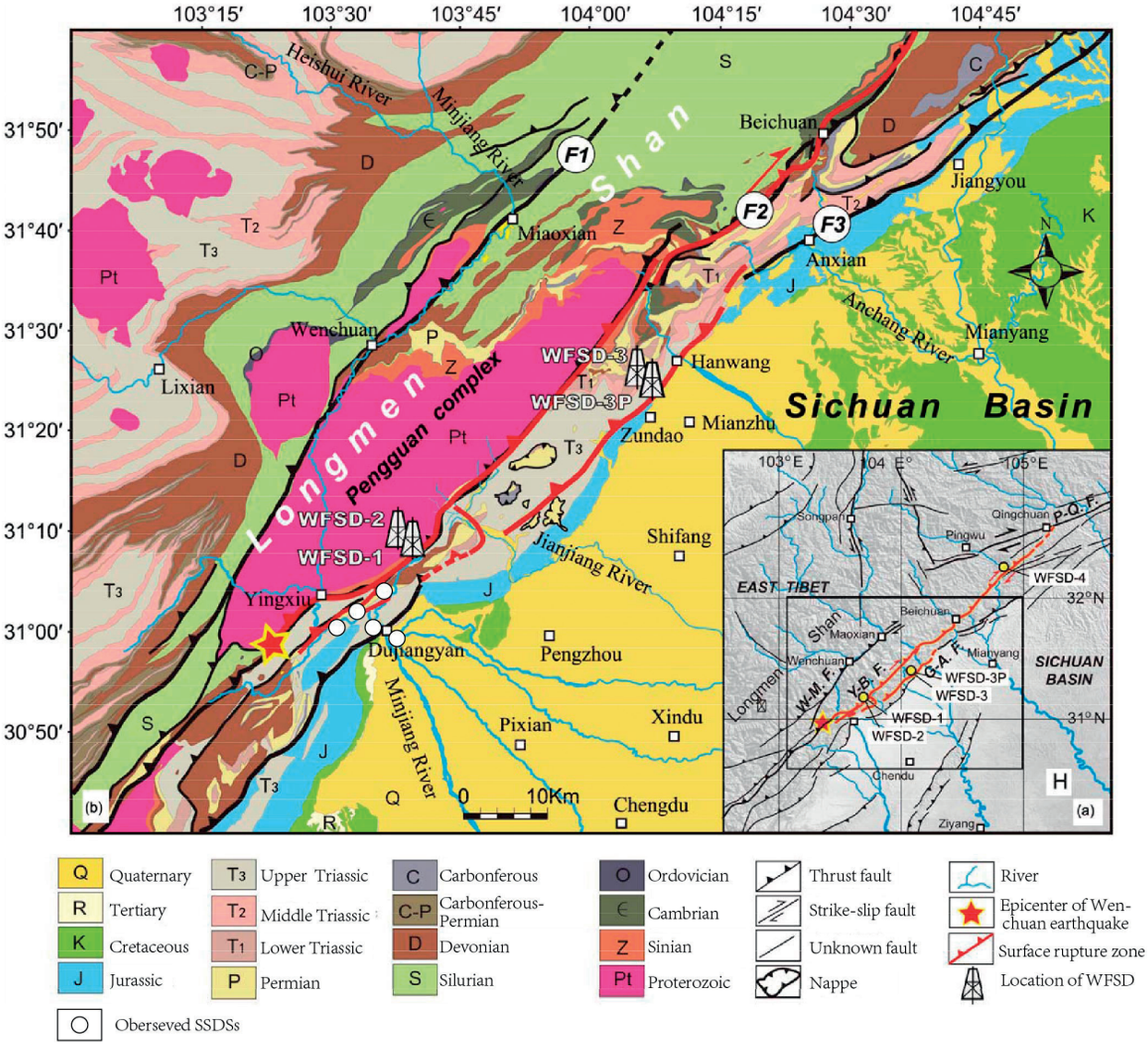

Figure 2. Simplified geologic and active tectonic map of the Longmen Shan and its adjacent area (adapted from 1:500,000 geologic maps, Ministry of Geology and Mineral Resources, 1991; [36, 37]) and observed SSDS sites during post-disaster investigation soon after the Wenchuan earthquake. F1, Maoxian-Wenchuan Fault; F2, Yingxiu-Beichuan Fault; F3, Anxian-Guanxian Fault.

and low-angle thrusts in the Longmen Shan, respectively [36–38]. The largest surface vertical displacements were attained at 12 m in the northern segment in the Beichuan area [39, 40]. There also occurred several soft-sedimentary deformation structures in the YBF and the terraces of the Mingjiang River, including liquefaction, gravitational and hydroplastic deformations and other related deformations. There is a need to mention that most SSDSs were observed soon after the Wenchuan earthquake had disappeared or been destroyed, because these SSDSs were distributed in the farmlands, river terraces or lawn and sandy areas of town. Prof. Li Haibing, one of the authors of this paper, pays attention to the liquefaction of sand deformations during the investigation of the Wenchuan earthquake in Longmen Mountain and its adjacent area, and makes a preliminary study on the soft-sediment deformation shortly after earthquake.

3.1.1. Sand volcanos and liquefied mounds

Various sand volcanos and liquefied mounds (**Figure 3**) have been observed in the Mingjiang terraces and adjacent areas of the Yingxiu-Beichuan Fault. They possessed different shape styles and internal sediment compositions. Unconsolidated saturated sedimentary sand layers are liquefied and flow upwards along vertical conduits and form mound-shape uplifts on the surface when the shaking occurred. The underground sands and gravels are brought by extrusion liquefied sand flow to the surface, and they form sand cones (**Figure 3D**) or gravel mounds (**Figure 3C** and **E**). Some of them are ejected out of the liquefied sands completely and form the craters (**Figure 3A**). Liquefied sand cones and gravel mounds usually occur in line along the Yingxiu-Beichuan faults (**Figure 3C** and **D**). The gravel mounds or cones are 1.5 m in diameter and 0.5 m high. If the thin gravel layer is covering the liquefaction layer, the upward sand flow entrainment gravels can form larger mounds. The largest one can reach 3.5 m in diameter and 1.5 m high. There are also small sand cones, which are parallel with the large mounds.

3.1.2. Liquefied sheet sands and collapse pits

Multiple liquefied sheet sands in a large area accompanied by ground fissures occurred in the Mingjiang terraces during the 2008 Wenchuan earthquake. The trending of ground fissures are parallel or perpendicular to the terrace margin, and the two groups of ground fissures constitute the netlike fissures. The underground liquefied sand flowed upwards and overflowed along the fissures to form the liquefied sheet sands (**Figure 3B**). The liquefied sheet sands also occurred from ring and radial cracks along the low sand dune.

There were many linear collapse pits in the farmland (**Figure 3F** and **G**), and the orientation of arrangement was usually paralleled to the Yingxiu-Beichuan Fault. They resulted from the liquefied sand dunes. The underground liquefied sand upwelling towards the ground, due to the process of liquefaction, ceased; the density of local underground layers changed to smaller; the sediments changed looser, even the underground caves occurred; and the collapse pits were formed due to downwards suction. Some undeveloped collapse pits also have the ring and ring and radial cracks (**Figure 3F**).

Figure 3. Sand volcano, liquefied dune, sand sheet, liquefied deformation of sand bed, triggered by May 12, 2008 Wenchuan earthquake (photographed by Li Haibing). (A) Sand volcano in the terraces of Mingjiang river; (B) liquefied sand sheets in the terraces of Mingjiang river; (C) a higher liquefied sand mounds in the Yingxiu-Beichuan fault zone; (D) liquefied sand dunes distributed in the lineal arrangement and parallel with the fault trend of the Yingxiu-Beichuan; (E) a liquefied sand and gravel mound, the gravels have been carried over the top of mound; (F) collapse sink resulted from liquefaction; (G) linear arrangement of the collapse sinks, diameter of collapse sinks are about 80–90 cm, the orientation is also parallel to the Yingxiu-Beichuan fault, showing the orange colour dot line.

3.1.3. Formation mechanism of SSDSs' response to the Yingxiu-Beichuan activity

Sand volcanos, liquefied mounds and collapse pits are recognised in the earliest earthquake records. And the liquefaction and ejection of fluid induced by the big earthquakes are key to fluid escape structures (sand boiling and sand volcano), which are composed of gas (often sulphur emanations), water, mud and sand, and under unstable fluidization environments [14, 30]. Nichols's experiments demonstrated the lower part material was fluidized and was blocked by the overlying non-fluidization layer, and when the grain size is more than 15% compared to the overlying layers, the biggest ejections can be produced [41]. But in huge modern earthquakes, sand volcanos and liquefied mounds are published little: first, because it is smaller than the earthquake rupture zone; second, it is easy to be destroyed by human activities and cannot be preserved. The liquefaction mounds and other SSDSs induced by the Wenchuan earthquake are extremely valuable geological records. Liquefied sand dunes, sand volcanos and liquefied gravel mounds reflect the process of the liquefaction, and the size and driving force of deformation structures are increased largely.

The Wenchuan earthquake produced the Yingxiu-Beichuan fault and Guanxian-Anxian faults with the NE-trending NW-dipping occurred surface rupture on the Longmenshan Fault Belts and with dextral-slip thrusting [36, 37]. The Longmenshan Fault Belts are the main margin fault of the West Sichuan foreland basin to the Songpan-Ganze terrane, and it is activated since the Triassic. From the distance of observed SSDSs to the faulted belts, range from 5 to 30 km, induced that the reactivated faults and triggered fault is the Yingxiu-Beichuan Faults (see **Figure 4**). These liquefied gravel mounds and sand volcanos are the records of events of the activity of the Longmenshan Fault Belts, and it is a response to the Indo-Asia collision and eastern extrusion of the Qinghai-Tibetan Plateau terrane. The activities of the Longmenshan Fault Belt is a result of the stress that originate from the Qinghai-Tibetan Plateau terrane converging to the north and escaping to the southeast, which were driven by the continent-continent collision between the India and Asian continent.

3.2. Triggered by the early Jurassic earthquake activities of the Talas-Ferghana strike-slip fault (TFSSF)

3.2.1. Soft-sediment deformation structures at the southeast end of TFSSF

Talas-Ferghana strike-slip fault has been active since the Mesozoic, but the initial time of strike-slip is still in dispute [42–44]. The Wuqia pull-apart basin of the Lower Jurassic was controlled by this huge fault (**Figure 5a**), with NW-trending, which is located at the south-east end of the significant Talas-Ferghana fault, SW Tianshan. Soft-sediment deformations were preserved in sandstone layers at top of the Lower Jurassic Kangsu Formation, and three earthquake-induced deformation sequences have been recognised within 10 m thickness of sandstones deposited in the lacustrine environment (**Figure 5b**). They are included as load cast, ball-and-pillow, droplet, cusps, homogeneous layer, and liquefied unconformity.

Load casts and ball-and-pillow are the main types of deformation in the third layer of SSDSs in the Kangsu formation. The parental sand layer providing load casts to subside is 80-cm-thick laminated siltstone and consists of limonite debris, feldspar, quartz and muscovite. The

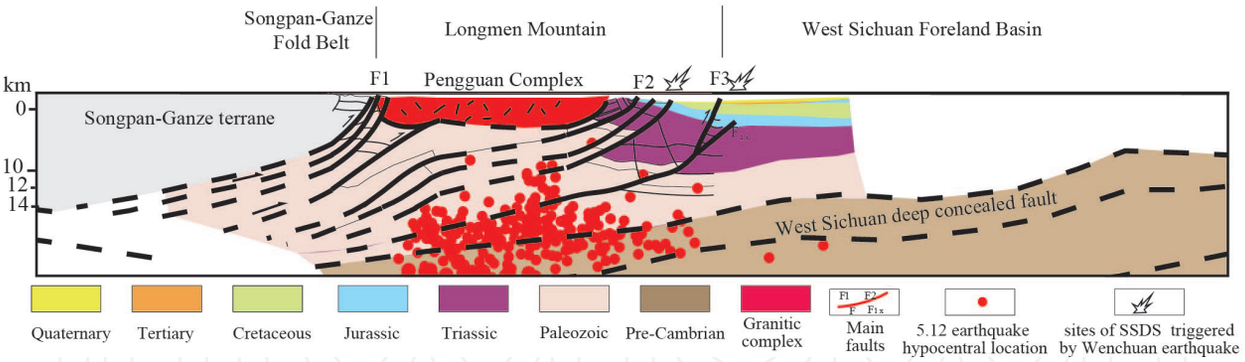

Figure 4. Sketch tectonic model of the Longmen Mountain and Sichuan Basin (modified from [47]), showing the main fault belts and 5.12 earthquake hypocentral locations and SSDS triggered by this earthquake. F1, Maoxian-Wenchuan Fault; F2, Yingxiu-Beichuan Fault; F3, Anxian-Guanxian Fault.

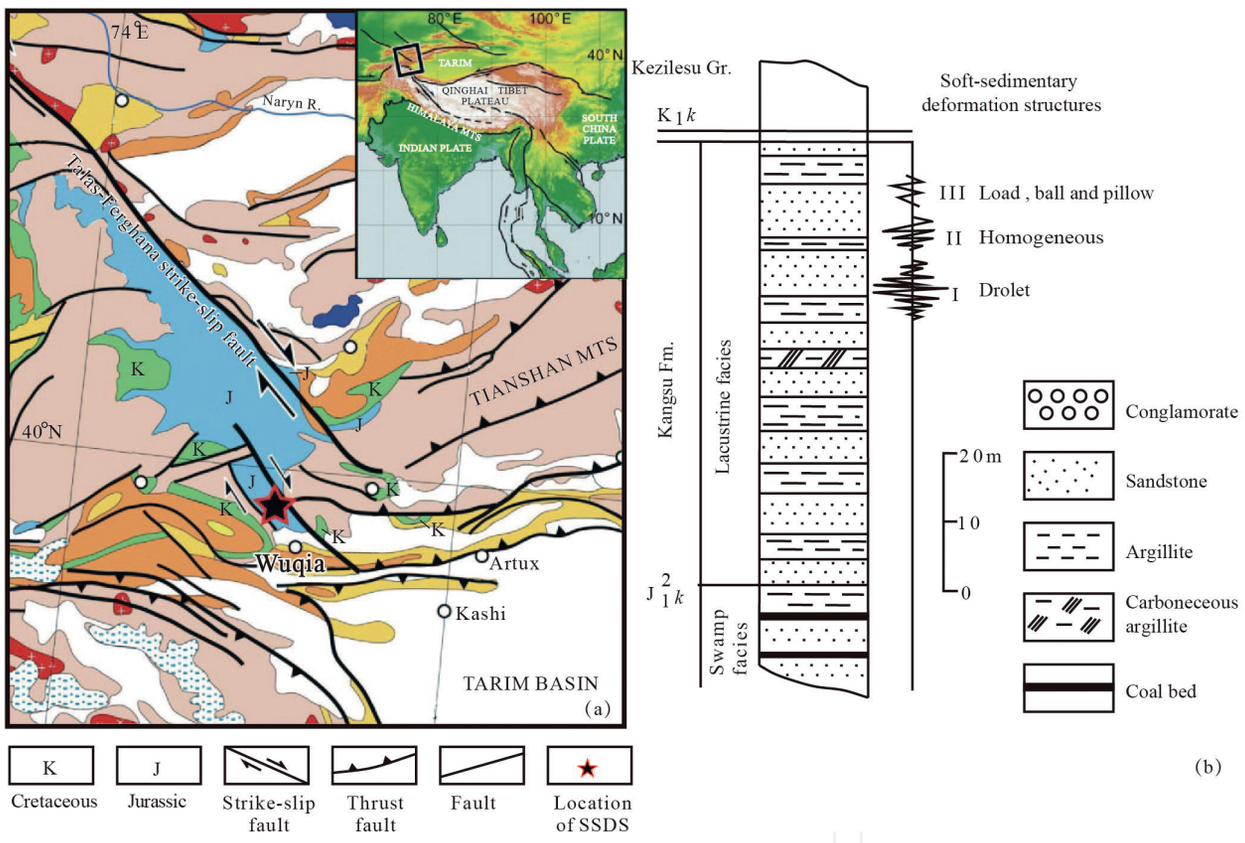

Figure 5. Geological sketch map (a) and stratigraphic column (b) showing the Wuqia Basin, southwest Tianshan Mts., Xinjiang (modified from [20, 47, 48]), and location of the SSDS in the Kangsu Formation in Jurassic. I, II and III presented the three layers of seismic events and composed a paleo-earthquake episode. The star marks the positions of these layers.

grain sizes range from 0.01 to 0.05 mm, with minor less than 0.5–0.1 mm, displaying distinct feature of seasonal lacustrine lamination (**Figure 6A** and **B**). The deformation structures resulted from the static pressure of the unconsolidated silt beds that were destroyed while

http://dx.doi.org/10.5772/intechopen.72941

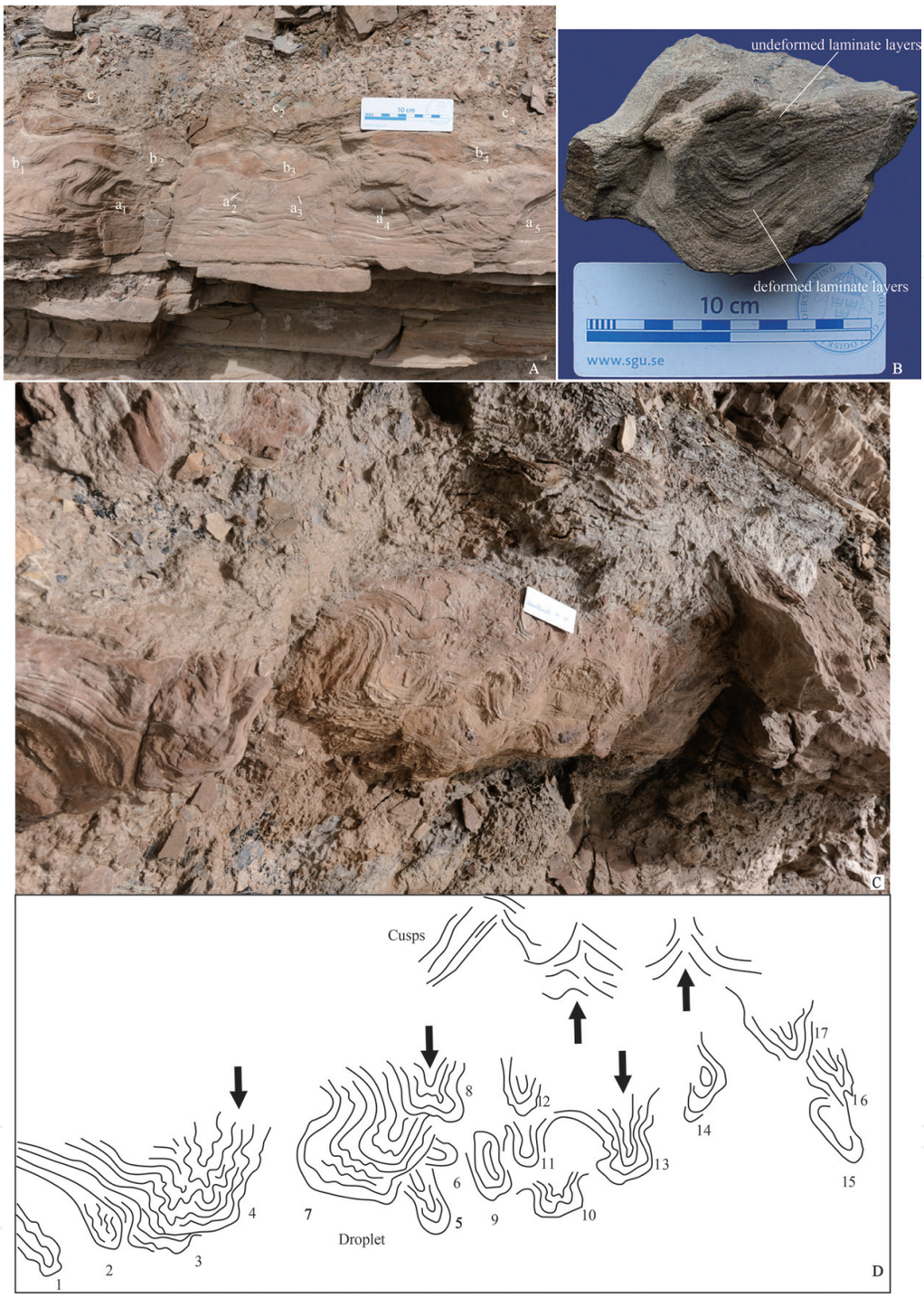

Figure 6. Soft-sediment deformation structures in the Kangsu Formation, Wuqia Basin, Southwest Tianshan Mountains. (A) Load cast and ball-and-pillow in the third layer of seismic event; a, b and c represent orders of load cast structures submerged. a_3 displays spindle, concentric laminae in ball-and-pillow. a_4 shows the intact stereo configuration of ball-and-pillow (oblate ellipsoid body). (B) Load cast showing syncline-like laminated layers resulted from subsidence of sand beds. (C and D) Long section morphology of droplet and upward cusps in the first layer of seismic event; arrows mark the directions of liquefying movement.

shaking, and gravity differentiation took place and sands or silts (the denser material) sank into the underlying (less dense) mud beds to form load-cast structures that evolved into 'ball-and-pillow structures' or pseudonodules [28, 32, 35].

Droplets and cusp anticlines occurred in the first event layer, about 60-cm-thick sandstone layer, of the Kangsu formation. Droplets and cusp anticlines resulted from strongly liquidised sandstone grains migrated vertically up and down during earthquake [45]. Seventeen intensively-distributed droplets can be seen within a distance of 170 cm along the sandstone layer (**Figure 6C** and **D**). They are revealed as cylinders and drops, with elongated U-type synclines in vertical cross sections and wavy laminates, presenting the trace of liquefaction flowing. Directions of axial planes of syncline-shaped laminae in each droplet are out of order, upright, oblique and curve, suggesting that downward displacement of sand grains is random and without sliding of sand bodies on slope. Cusp anticlines are similar to diapirs in configuration of structures but different to diapiric structures. The diapiric structure refers to the underlying liquefied sand bed puncture into overlying soft sediments, while cusps are the result of liquefaction sands migrated upwards within liquefied sand layer with corn-shape body and without distinct xenolith in nucleus (**Figure 6C** and **D**). Droplets and cusp anticlines are formed under the duel effects by liquefaction and gravity. Groups of droplets resulting from superimposition of droplets and cusp anticlines resulting from upward movement of liquefying sandstone constitute multilayer complex deformation layers, which are generally explained to be triggered by earthquakes.

3.2.2. The activity of Talas-Ferghana strike-slip fault during the late early Jurassic

Three deformation layers of the Kangsu formation in the Lower Jurassic in Wuqia Basin had differences of deformation mechanisms (**Figure 5b**). The first deformation layer was characterised by droplet and cusp structures resulted from vertical liquefied displacement; the second was mainly homogeneous layers of liquefied sands and local unconformity and the third was mainly load casts and ball-and-pillow resulted from the effects of gravity and seismic shaking. Therefore, three seismic events suggest that the Talas-Ferghana strike-slip fault zone occurred due to at least three times large-scale active events during the late early Jurassic, with the different paleo-stresses imposed on soft sediments and made them deformed. According to the recorded data of liquefaction of sand layers by modern earthquakes and previous earthquakes [20, 30, 46], the SSDS were 45 to 50 km away from the Talas-Ferghana fault, and Ms 6.5–7 of the paleo-earthquake magnitudes were estimated.

3.3. Triggered by the early Palaeozoic activities of interior faults of the Tarim Basin

3.3.1. SSDSs in the deep drilling cores in the Manjiaer depression and Tazhong uplift

Tarim Basin is the largest, very complex, oil-bearing, superimposed marine facies and continental facies basin (560,000 km^2), in north-western China. It is surrounded by the Tianshan-Beishan, West Kunlun and Altyn Tagh mountain belts to the north, south, and southeast, respectively (**Figure 7**). The basin has undergone a long geological evolution with multi-phase tectonic movements from the Neoproterozoic to the Quaternary. The

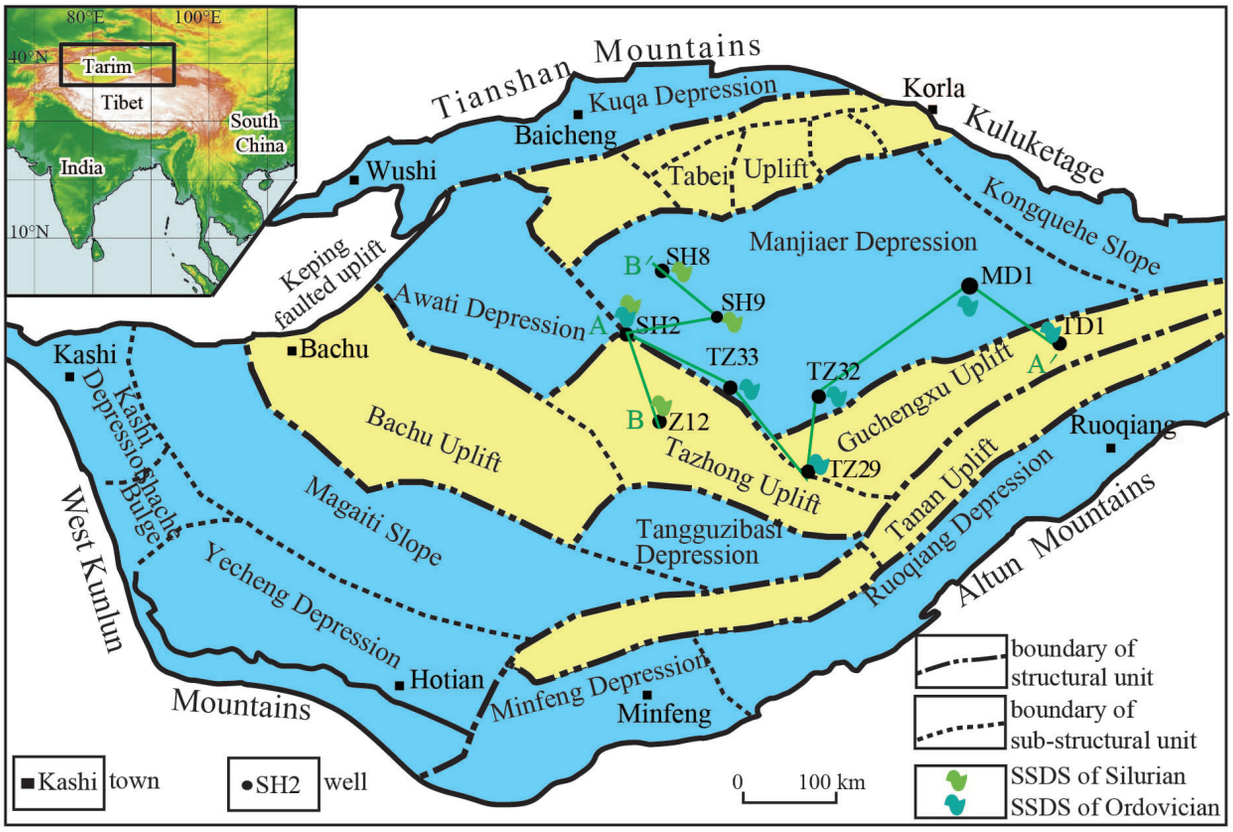

Figure 7. Schematic map of the structural units of the Tarim Basin, showing the location of deep drilling wells in Tazhong uplift and Manjiaer depression, in which various SSDSs of the Ordovician and Silurian are observed.

early Palaeozoic is the main period of development, especially in the central parts of the basin. During the first tectonic cycle, which is from the latest Neoproterozoic to the Middle Devonian, two unconformities that are Silurian/Upper Ordovician and Upper Devonian-Carboniferous/pre-Upper Devonian unconformity were formed during the middle and late Caledonian tectonic movements [49–53]. The properties of main faults changed from the normal faulting to reverse faulting during the middle Caledonian movement. The paleo-tectonic activities of this area are key issues and remain enigmatic for understanding the basin reconstructions and hydrocarbon explorations.

From the Ordovician to Silurian, the sedimentation (**Figure 8**) took place in a marine basin facies, shelf-and-platform (**Figure 8b**) and tidal-flat facies (**Figure 8a**) depositional environment in the Tazhong Uplift and the Manjiaer Depression. Various millimetre-, centimetre- and metre-scale soft-sediment deformation structures (SSDSs) have been identified in the Upper Ordovician and Lower-Middle Silurian from deep drilling cores in the Tazhong Uplift and the Manjiaer Depression (**Figure 7**). They include liquefied sand veins, liquefaction-induced breccia, boudinage-like structures, load and diapir- or flame-like structures, dish and mixed-layer structures, hydroplastic convolutions and seismic unconformities (**Figure 8**). They were commonly mistaken for worm traces, mud cracks or storm deposits since they have abrupt contacts with the surrounding sedimentary rock (according to the geological well reports).

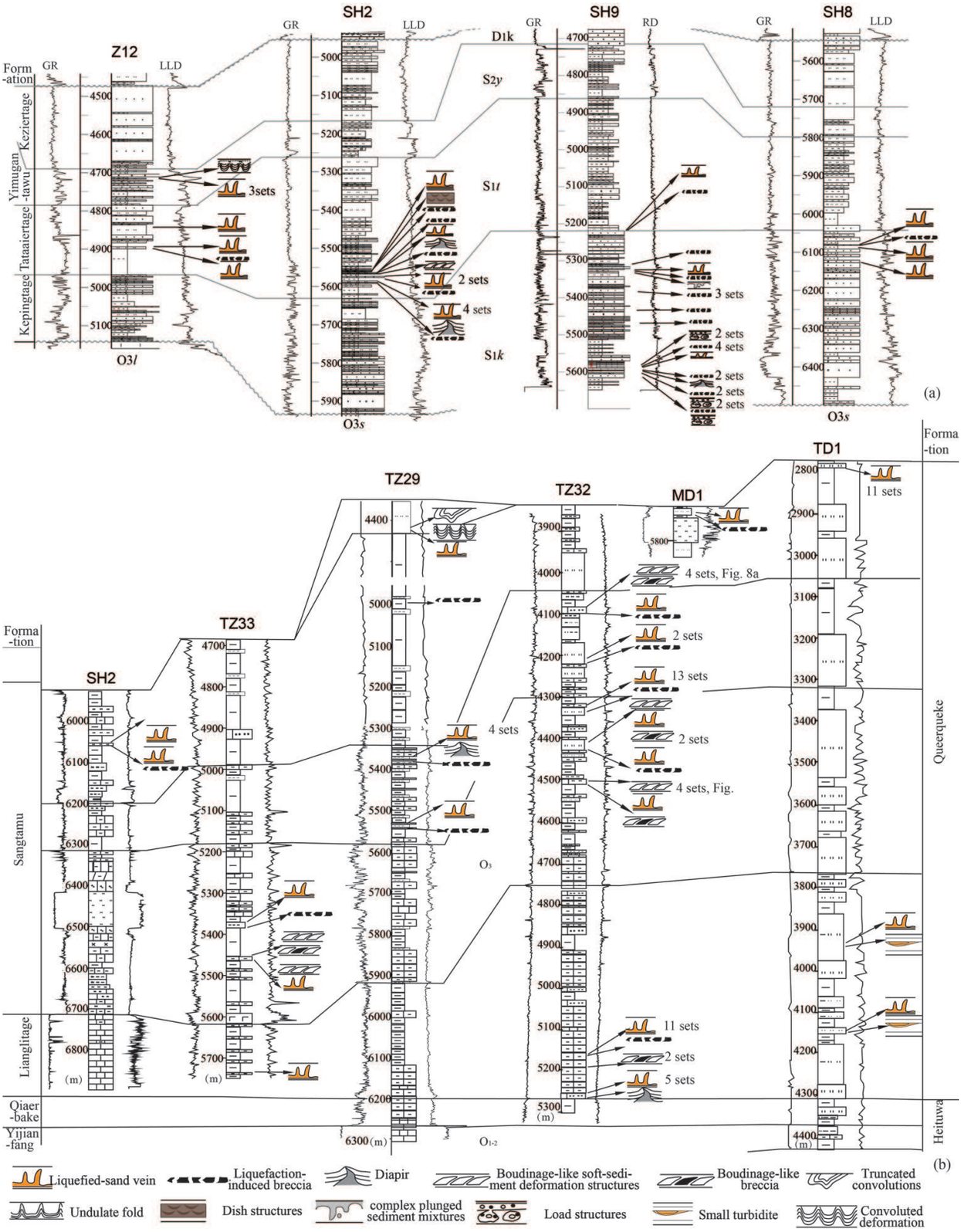

Figure 8. Correlation of strata and paleo-seismic records in the Silurian (a) and Upper Ordovician (b) in the central part of the Tarim Basin (modified from [54]), showing the types and layers of observed SSDS.

http://dx.doi.org/10.5772/intechopen.72941

3.3.1.1. Liquefied sand veins and liquefaction-induced breccias

Liquefied sand veins are common in the studied cores and have been identified in many wells (**Figure 8**). These liquefied sand veins are a vein-type structure that is formed by injection of liquefied sand flow. Unconsolidated near-surface sands that are water-saturated may liquefy when are abruptly loaded or shaken. This results in overpressure of the pore water, which may then escape to adjoining lower pressure intervals by forming injection features in otherwise undisturbed deposition. Liquefied sand veins in the MD1, TZ29, SH2 and Z12 wells range in width from 2 mm to ~ 3 cm and their length ranges from 1 cm to over 10 cm. They consist of laminated thick horizontal mud layers interbedded with thin silty or fine sand layers, the grey silty sand liquefied and emplaced grey black mud beds. Liquefied sand flows have two occurrences: vertically liquefied (**Figure 8B**) and lateral liquefied (**Figure 9A**). The veins are irregularly curved, with bifurcation in cross section, and without a uniform planar direction as plate in 3D morphology. The textures and components of the sand veins are similar and differ obviously from the surrounding mudstones. Liquefied sand veins cut through mud beds and trigger arching or concave bending (**Figure 9A**, **D** and **E**) of the surrounding laminated mud beds. Thin interbedded sand and mud can form multilayered, interpenetrated and complex vein, like the liquefied sand veins of SH2 well on Silurian composed of ochre sands (fine sands or silty sands) liquefied and invaded in the over- and underlying brown muds. Some of the liquefied sand veins are associated with liquefaction-induced breccias.

Liquefaction-induced breccias are produced by liquefaction of sands that are both overlain and underlain by mud layers. Liquefaction of the sand causes disruption of the surrounding mud beds into gravel-sized, clayey breccia fragments. Liquefaction-induced breccias occur together with liquefied sand veins (**Figures 9A** and **10A**). Grey silty gravels were confined by black grey mudstones; breccias are components of grey green silty mudstones and siltstone fragments with angular and assorted sizes of gravel particles ranging from 0.3 to 1 cm. Such breccias have been interpreted as genetic of storm flow (taken from the final well report) by the mixed and disorderly sedimentary breccias intercalated into the undeformed stable layers. However, the breccias were formed in the mud layers by invasion, ripping up and truncating by liquefied sand veins. The breccias are in-situ and non-transportation. **Figure 10D** shows a liquefied gravel-bearing sand veins and a micro-thrust fault coexisted deformation structure.

3.3.1.2. Boudinage-like SSDS and boudinage-like breccias

Boudinage-like soft-sediment deformation structures (BSSDS) are for the first time identified in the Upper Ordovician in Manjiaer depression and the metre-scale deformation structures in vertical stratigraphic sequences. They consist of thin, light grey calcareous siltstones interbedded with dark grey calcareous mudstones deposited in mixing siliciclastic and carbonate shelf environment. The unconsolidated sediments under horizontal shear stress form boudinage-like structures, rapid depositing sediments with large thicknesses and undeform layers with similar properties on lithology and sedimentary intervals. Multiple cycles of BSSDS are identified in the TZ32 and TZ33 wells (**Figures 8B** and **9B**). The calcareous sand beds with

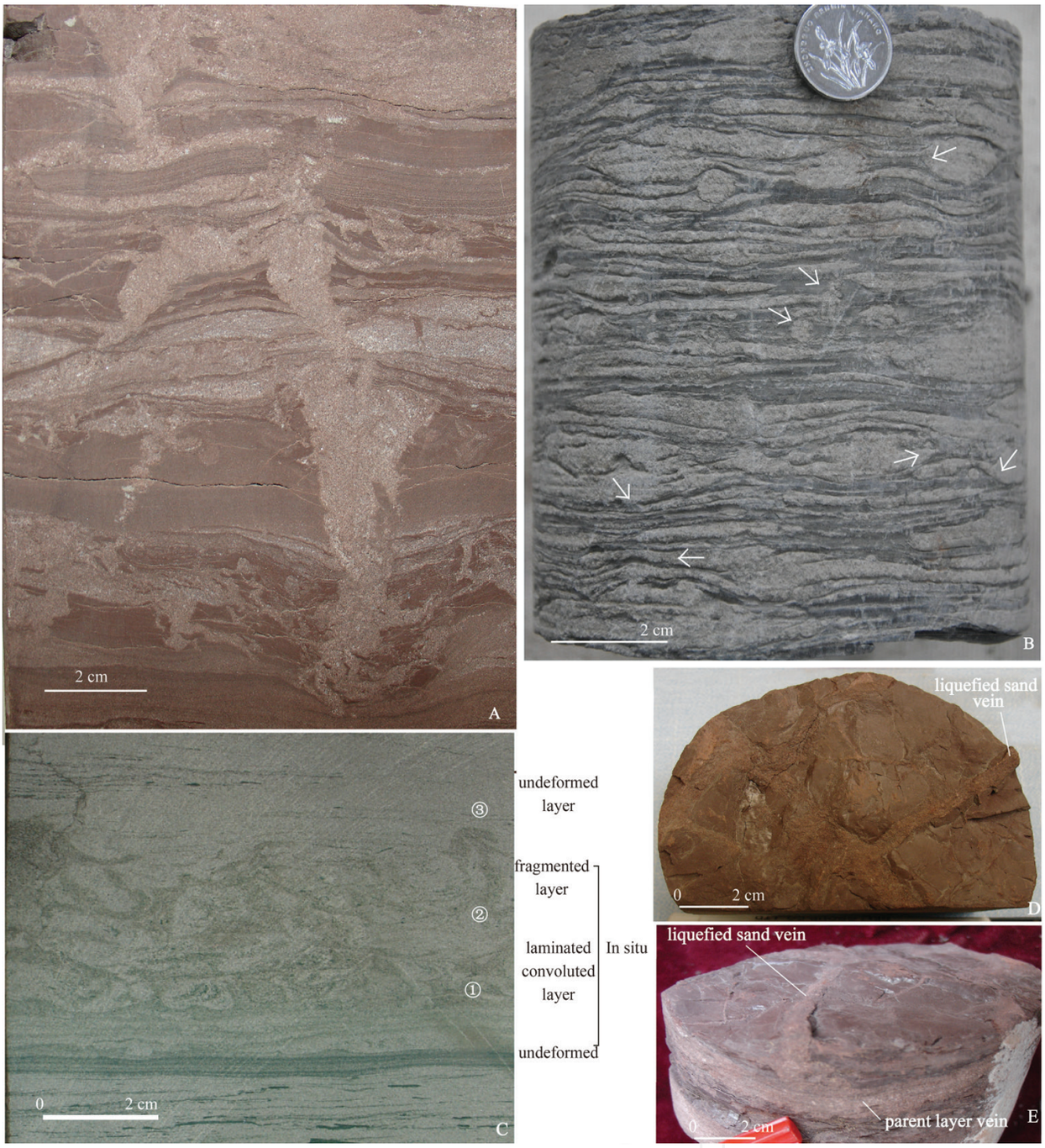

Figure 9. Typical SSDSs in the deep drilling cores (1), in the central part of the Tarim basin. (A) Concentration of sand veins, well SH2, depth 5567.3 m; Yimugantawu Formation of the Middle Silurian (S2*y*). (B) Boudinage-like soft-sediment deformation structures (B-SSDS) and small liquefied sand veins, well TZ32, depth 4507.5 m, Upper Ordovician. (C) Mixed-layer structures, well Z12, depth 4713.8 m; Yimugantawu Fm. Of the middle Silurian. (D and E) Sand veins in cross section and plane, well SH2, depth 5573.1 m; stratigraphical unit S2*y*.

comparatively higher cohesive muds were sheared and cut off, to form lenticular sand bodies under tensional shear stresses.

3.3.1.3. Plunged sediment mixtures

Plunged sediment mixtures refer to the deformation that occurs near or on the boundary between two different unconsolidated stratigraphic units [54]. These two units usually have

little difference of the upper and lower sediments. The discontinuous undulate surfaces are easily produced at the boundary, and the sediments of the upper unit form ground fissure, load cast, ball-and-pillow at the top of the lower unit. Spherical, mushroom-shaped and ellipsoidal bodies (**Figure 10B**) of the lower unit also invaded the upper unit by liquefaction and diapirism.

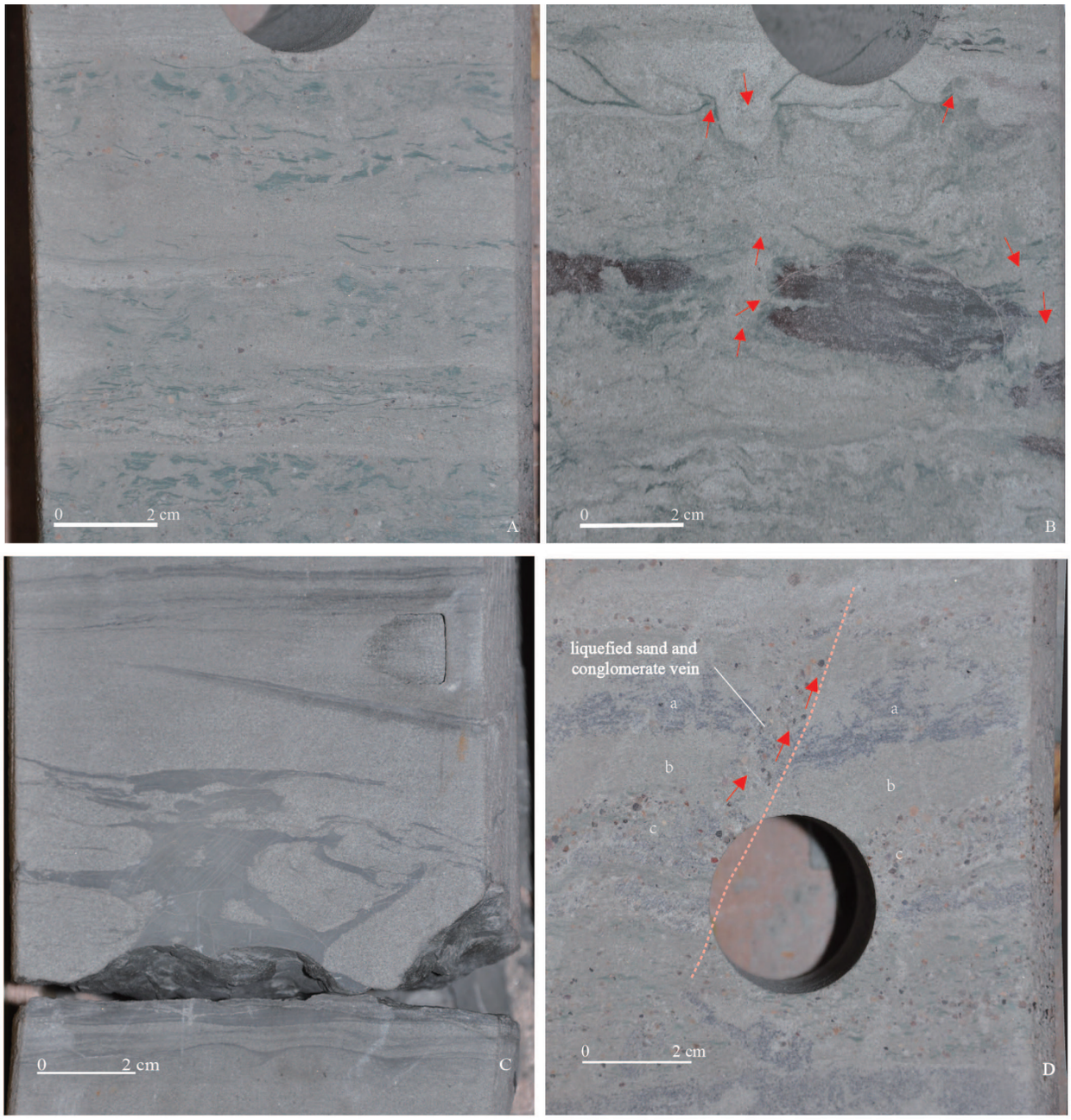

Figure 10. Typical SSDSs in the deep drilling cores (2) of Kepingtage Formation of the Lower Silurian, in well SH9, central part of the Tarim basin. (A) Liquefied breccia and liquefied sand veins, dark grey muds were brecciaed vertically or horizontally by light grey silts emplaced, depth 5590.15 m. (B) Complex plunged sediment mixtures, the wavy interface and load cast were formed, with some light sand layers and light celadon liquefied sand veins, depth at 5342 m. (C) Thixotropic diapir, showing that the dark grey muds experienced thixotropy upward movement to the upper light grey silt sands and formed diapir structures, which were intercalated by the overlying and underlying non-deformation flatting dark grey mud layers and light grey silt layers, showing a complete non-seismic, in-seismic, and non-seismic sequence vertically; well SH9, depth 5606 m. (D) Liquefied gravel-bearing sand veins and a micro-thrust fault, liquefied light grey sand with brown fine gravels and cut the laminated grey mud layer, and superimposed by mini-type thrust fault, depth 5339.69 m. Red arrows indicate the orientation of rheology of particulate matter.

3.3.1.4. Thixotropy wedge and diapir

Thixotropic wedges usually develop in fine-grain sediments, which are thixotropic flow deformation triggered by an earthquake activity [14, 20]. While the soft sediments (mud, soft siliceous sediment and carbonate ooze) with the grain size are less than 0.005 mm, the strength of fine-grain sediments and clays decrease owing to seismic shear stress effect, resulting in the complex rheological phenomenon that occurs (**Figure 10C**). Three axis vibration test of saturated soft soil presents when the seismic intensity is 7 or greater (amount to the earthquake magnitude is 5.6), and muds usually do not be liquefied but it happens with thixotropic flow, which is triggered by shocking [55, 56]. The earthquake magnitude for thixotropic deformation is higher than liquefied deformation [57]. Many deformation structures in argillaceous rocks, silica rocks and micritic of carbonate rocks can be interpreted by the thixotropic mechanism (**Figure 10C**).

The wedges may be very narrow and are recurrent. Thixotropic wedges are obviously different with the ground fissure in hard rock layers. Thixotropic diapir indicates that mud layers flow upwards with thixotropy owing to shock and intrude or emplace in the fine sand or silt layers (**Figure 10C**).

3.3.2. SSDSs triggered by the paleo-activities of the Tazhong 1 and secondary faults

During the late Ordovician to early Silurian, the Tarim Basin underwent conversion from a tensional to a compressive flexural tectonic environment. Accompanied by the Proto-Tethys Ocean subducted in a northward direction since early Ordovician [58], the middle Kunlun terrain collided with the Tarim plate and the South Altun Ocean closured during the late Ordovician [59, 60]. The southern parts of the Tarim Basin was the strong deformation area, especially the southeast area [52, 53], and the main faults in the Tazhong uplift and Tangguzibas depression were activated strongly (**Figure 11**) and responded to the orogenic activities. The NW-trending Tazhong 1 fault (TZ1F) was the boundary fault between the Tazhong Uplift and the Manjiaer Depression during the late Ordovician to Middle Devonian and the paleo-active strength of fault movement was strongest during the Ordovician, with a vertical fault displacement in excess of 2 km (**Figure 11a** and **c**). The property of the TZ1F changed from the normal fault to the reverse fault at the end of the late Ordovician. The west segment of TZ1F ceased activity before or in early Silurian depositing, and the middle and south segments remained active to the early Carboniferous. The activities of the secondary reverse faults of the TZ1F were dominated during the Silurian. At the same time, a series of NE-trending small faults were active but the displacements were little (**Figure 11b**). The normal and strike-slip property of these small faults had been recognised in the 3D seismic data.

These SSDSs, which are intercalated by undeformed layers with similar lithology and sedimentary facies, are observed with wide distribution near the faults (**Figures 7, 8** and **11**). So the SSDSs resulted from the bursting events after they were deposited but incompletely consolidated. Most of them (Well SH2, TZ33, TZ29 and TZ32) in the Upper Ordovician are in the drilling cores nearby the TZ1F and a little in the farther wells (MD1 and TD1). About 51 layers of SSDSs have been observed in the 1500 m sedimentary layers of the Upper Ordovician (deposited during 447–444 Ma) and 26 layers of SSDSs have been observed in about 800 m sedimentary layers of the Lower Silurian (deposited during 436–421 Ma) (**Figure 11c**).

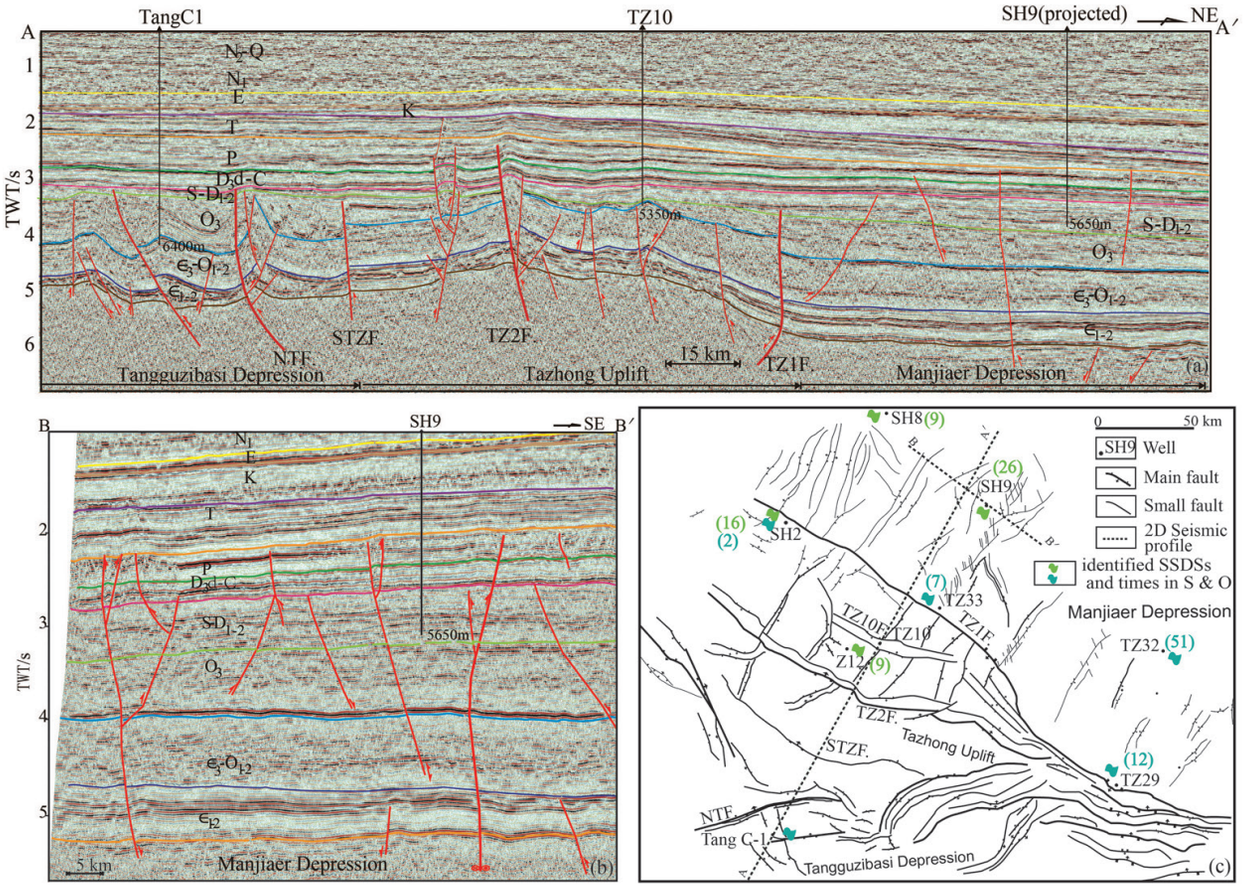

Figure 11. 2D seismic interpretation profiles of the Tazhong uplift and its adjacent area (A-A′, B-B′), (c) the fault systems of the Silurian in the Tazhong uplift and its adjacent areas (modified after Northwest Oilfield Company of SINOPEC, 2015), showing the identified seismic event layers in the deep drilling cores.

Based on their characteristics, the inferred formation mechanism and the spatial association with faults, the SSDSs were triggered by the paleo-active NW-trending TZ1F and a series of NE-trending small faults. The TZ1F was a seismogenic fault during the late Ordovician, whereas the reversed-direction secondary faults and multiple small NE-trending faults were the seismogenic faults in the Early-Middle Silurian. The SSDSs triggered by the paleo-active faults may be represented as records of the high-frequency tectonic events with the pulsation and circularity during the main tectonic movement phases.

3.4. Triggered by the Mesoproterozoic earthquake activities in the northern margin of the North China Craton

3.4.1. SSDSs of the Mesoproterozoic in the Yan-Liao Aulacogen

The SSDSs of the Mesoproterozoic in the Yan-Liao Aulacogen, which is located in the northern margin of the North China Craton, were recognised first by Song [62], and the oldest SSDSs have been observed in China [61–63]. In the Chuanlinggou and Gaoyuzhuang Formation of the Changcheng System (1800–1400) and Wumishan Formation of the Jixian

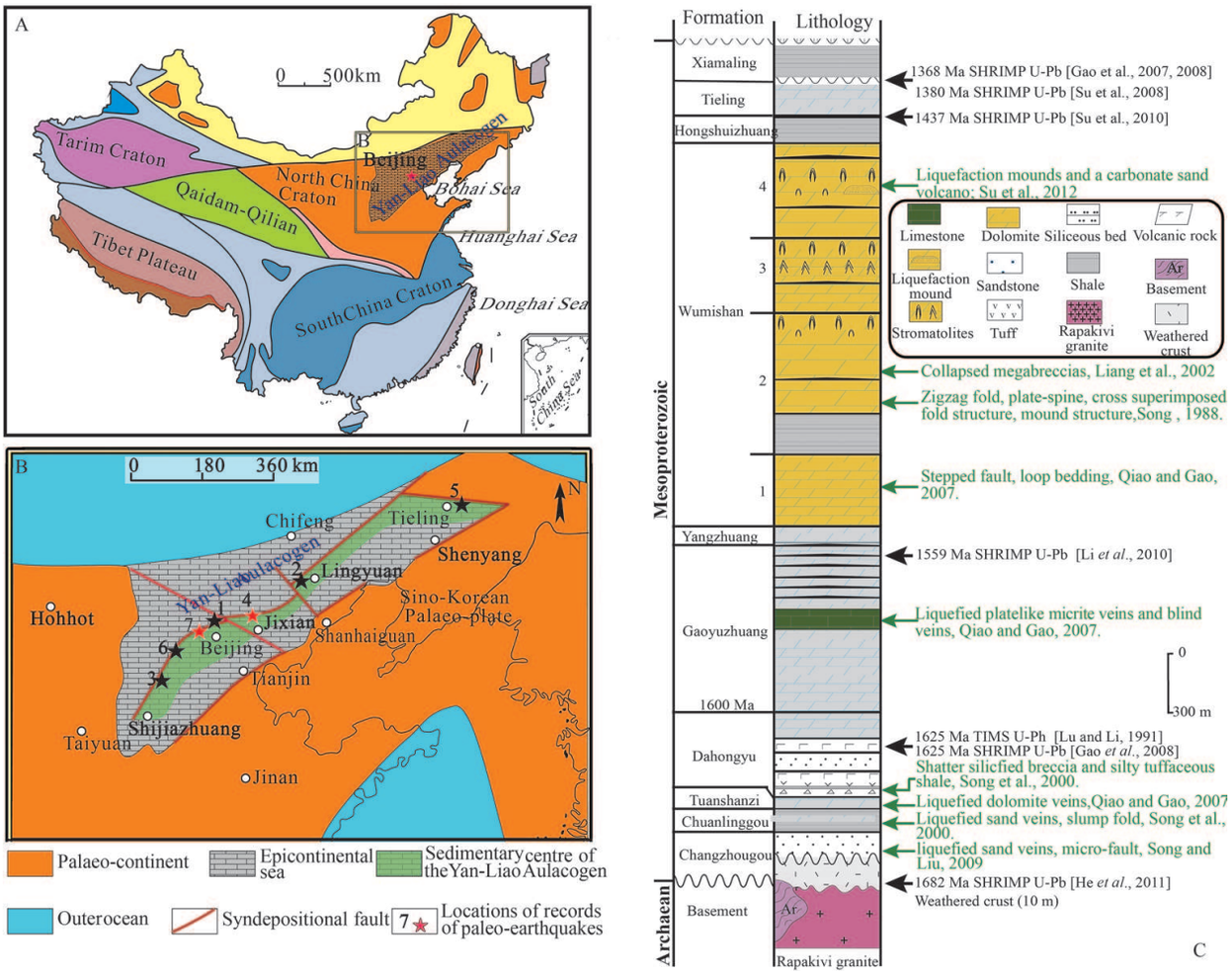

Figure 12. (A) Paleo-plate sketch map of China, showing the distribution of the major paleo-plates of different ages (after [62]). (B) Paleo-geographical map of the Yan-Liao Aulacogen from the Proterozoic Gaoyuzhuang Stage to the Wumishan Stage showing an epicontinental sea opened to the north, and the approximate positions of the discovered seismites (after [63–66]). The identified outcrops of earthquake-triggered SSDSs are marked by stars, 1—[60]; 2—[67]; 3—[68]; 4 and 5—[64]; 6—[32, 69]; 7—[66]. The red stars show the position of the seismites in this paper. (C) Lithostratigraphy of the Mesoproterozoic of the Yan-Liao Aulacogen (modified from [66–74, 77–79]), the records of multiple paleo-earthquake events in green words and volcanic events in black words are shown.

System, various SSDSs have been observed, which mainly developed in the epicontinental sea (**Figure 12**). They are liquefied sand veins, liquefied carbonate mounds, liquefied breccia, hydroplastic deformation, various curly deformation, looping bedding and graded faults. Deformed layers are separated by the undeform layers. The SSDSs in the Chuanlinggou Formation are composed of clastic rocks in the intertidal and subtidal environments, and the others are composed of carbonate rocks deposited in carbonate platform (**Figure 12C**).

3.4.1.1. Liquefaction mound and carbonate sand volcano

They are typical SSDSs in the Wumishan Formation (1550–1400 Ma) of the Mesoproterozoic, with the mound and crater in shape (**Figure 13a–c**), linear arrangement along a roadcut near Zhuanghuwa Village, ca. 70 km west of Beijing. Liquefaction mounds have generally

http://dx.doi.org/10.5772/intechopen.72941

Figure 13. Typical seismites triggered by the Mesoproterozoic earthquakes in the Yanliao Aulacogen, the northern margin of North China Craton. (a) Linear distribution of liquefied carbonate mounds of the Wumishan Formation, the orientation of mounds paralleled to the trending of the Shijiazhuang-Lingyuan Fault of the Yanliao Aulacogen, spot 7 illustrated in **Figure 12**. (b) Close-up views of mound 1 at the Zhuanghuwa sections, note the concentric circular rings and the radial fissures (arrowed). (c) The fine-grained carbonate-sand volcano of the Wumishan Formation, Zhuanghuwa section, spot 7 illustrated in **Figure 12**. (d) Loop bedding of the Wumishan Formation in Yongding River Valley, Beijing. (e) Netlike liquefied dolomite veins and argillaceous dolomite breccia, Tuanshanzi Formation, spot 4, Tuanshanzi village, Jixian, Tianjing. (f) Plate-spine breccias and intense folds, algal dolostones, Wumishan Formation, in Yongding River Valley, Beijing.

rounded shapes, with some concentric and radial fissures. They are composed of grey dolostone with minor amount of black siliceous (chert) rock, especially on the top of the mounds. The diameter of the mounds varies between 1.5 m and 4 m and their height from 10 cm to 30 cm. **Figure 13b** shows the best-exposed mound has an almost perfectly circular shape, with a diameter of 2.8 m, 6 concentric circular fissures and 13 radial direction

fissures. The fissures are filled with dark siliceous chert rock. A carbonate sand volcano also remains, which is shaped just like a small volcano with a crater (**Figure 13c**). It has a diameter of 110 cm and a thickness of about 30 cm. And a thin layer of black siliceous rock is built up in the centre of the depression. There are also at least three (possibly five) radial fissures exposed, which are filled with dark siliceous material.

3.4.1.2. Loop bedding

Loop beddings are ductile deformation structures, which consist of lacustrine finely laminated sediments and are induced by extension stress, presented as loops or chains (**Figure 13d**), and the adjacent layers are undeformed. In the Wumishan Formation of the Mesoproterozoic near Yongding River Valley, they are formed in a deep-water carbonate platform setting and suffered the horizontal shear stress. Loop beddings can be also formed in epicontinental seas and a low energy environment below the wave base of marine settings [66, 72, 76]. It is a result of stretching from unlithified to progressively lithified laminated sediments in response to successive minor seismic shocks, ultimately related to the slow movement of extensional faults [74, 75].

3.4.1.3. Intense intrastratal folds and plate-spine breccias

The strong intrastratal folds occur in the upper part of the Zhuanghuwa section and Yongding River Valley and are about 10–20 cm thick. They are deposited in a very shallow-water depositional environment indicated by the mud cracks and ripple marks beneath this deformed layer.

Plate-spine breccias are widely observed in lamellose or ribbon stripped layers of the Mesoproterozoic in the North China craton. These deformations are formed when the incomplete consolidated laminated layers experience continued compression and completely crack along the axial plane of folds. **Figure 12f** is a superimposed deformation structure of the intrastratal fold and plate-spine breccias, which are formed on two wings of folds, and the top of the fold layer without erosion looks like clouds and is covered by undeformed laminated layers. The formation mechanism of plate-spine breccias may be seismic activities [60]. Ettensohn et al. called the intense folds accordion-like folds, which are induced by earthquakes [34].

3.4.2. SSDSs triggered by the paleo-activity of the Shijiazhuang-Lingyuan Fault Belt

The Yanliao taphrogenic trough is a NE-trending rifting basin in the northern part of North China Craton and is open to the north [63–65]. The Shijiazhuang-Lingyuan Fault Belt (>800 km long) is the main fault belt with the NE-trending (**Figure 12B**), which is extended along the axial part of the Yan-Liao Aulacogen, activated during the early Mesoproterozoic in an extension tectonic environment [63]. The observed SSDSs are mainly distributed approximately less than 20 km from the fault in vertical distances. Identified SSDSs include intrastratal faults, liquefaction sand veins, liquefaction carbonate mounds and volcanos along the paleo-active fault belts. The SSDS layers have been interbedded by the many undeform layers. And some of them have the abnormal geochemical records such as Re, Os, Ir and other rare elements in black silty mudstones or shale of Chuanlinggou Formation that give a clue that volcanic and seismic events existed [77]. The liquefaction carbonate mounds and sand volcanos in the Mesoproterozoic have similar features which induced by the recent Wenchuan earthquake

(Ms 8.0) in Sichuan Province, SW China in 2008. According to the mechanism of SSDSs and the relationship of the activity of SSDSs and faults, they may be triggered by paleo-seismic events of the Shijiazhuang-Lingyuan Fault Belts. There are about 29 times deformation layers or seismic event layers have been observed in the Zhuanghuwa section, and the occurrence frequency of the strong paleo-earthquakes is about 20 thousand years to 32 thousand years [78, 79]. Multiple seismic events and activities of the Shijiazhuang-Lingyuan Fault Belt are responded on the break-up of the Columbian supercontinent.

4. Implication and prospects of the high-frequency tectonic events studied

4.1. Understanding the history of fault activities

The typical cases of seismites at different times in China reveal the sequence of paleo-earthquake events, and the activities of seismogenic faults can help us understand the dynamics of tectonic developments in different regions.

Seismites research may provide geo-history evidences for active seismic fault belts. The vertical sequences of paleo-earthquakes (seismites) are separated by undeformed sedimentary layers. They will provide a history of gradual and abrupt changes of the tectonic development and evolution in a particular region and regular patterns of seismicity of this region. Correlation of the paleo-earthquake activity sequences will help us to know spatial and temporal characteristics of paleo-seismic events in the main tectonic movement. This will provide important supplementary evidences of the impulsive and cyclicity of tectonism of the main tectonic movement. And they can also provide evidences for the tectonic records during a period from 10^2 to 10^6 yr (The white paper resulting from a workshop held at Denver Colorado, 2002), which is a difficult issue in the frontier research of structural geology and tectonic science. Paleo-earthquake events will build a link between orogenesis, high-frequency tectonism (in basin-mountain system) and a seismic activity.

4.2. Dating precisely of the tectonic events

Since seismites formed before sediments are completely consolidated, the age of depositing sediments in seismites could indicate the approximate time of a paleo-seismic event, and the ages of syn-depositional volcanism and organic debris in relative layers of seismites can provide evidence for the absolute age of seismicity and the tectonic events. The ^{14}C dating (radiocarbon dating), the U-Th disequilibrium technique (speleothem calcite), the electronic spin (ESR) (fossil dating), the K-Ar and ^{40}Ar-^{39}Ar dating (syntectonic illite) and the detrital zircon U/Pb dating (LA-MC-ICP-MS) can provide the different time-scale dating.

4.3. Effects on paleo-ecological environments and energy resources

Paleo-seismic research may help us understand more the changes of sedimentary paleogeographic and ecological on different scales. It is a new research direction to combine paleo-earthquake, which is an unexpected and catastrophic event, with life and environmental change.

He et al. analysed a host of identified Cretaceous seismites in Zhucheng faulted depression in Shandong Province, discussed the relationship between the distribution of seismites and the mass buried dinosaur fossils and pointed out that paleo-seismicity and environment change may result in migration of dinosaurs [80].

Faults and fractures can be channels for fluid flow, especially hydrocarbon migration and mineral accumulation in different times, but also as destroyers for them when the faults and fractures are active later. The paleo-seismicity accompanied by development of faults and fractures will affect the lithology, structural deformation, fluid properties, pressure-temperature and anisotropy of consolidated rocks. The research of intensity, frequency and distribution of paleo-seismic events help us to understand structural deformation, fracture development, characteristics of porosity and permeability and fluid migration. Integrated research of paleo-seismicity, basin structural and paleogeographic evolution may provide the reallocation and final determination of positions of oil and gas reservoirs and mineral resources.

Acknowledgements

This study was supported by the Science Research from the Northwest Subcompany of SINOPEC (no: KY2013-S-024), the work project of China Geological Survey (no. 12120115002001, DD20160169), a Special Research Grant from Ministry of Land and Resources of the People's Republic of China (no. 201011034), the Major Project of National Natural Science Foundation of China (no. 41630207).

Author details

Bizhu He*, Xiufu Qiao, Haibing Li and Dechen Su

*Address all correspondence to: hebizhu@vip.sina.com; hebizhu@cags.ac.cn

Key Laboratory of Continental Tectonics and Dynamics, Institute of Geology, Chinese Academy of Geological Sciences, Beijing, China

References

[1] Scholz CH. Earthquakes and friction laws. Nature. 1998;**391**:36-42

[2] Deng QD, Zhang PZ, Rang YK, Yang XP, Min W, Chu QZ. Basic characteristics of active structure in mainland of China. Science China (Earth Sciences). 2002;**32**:1020-1030 (in Chinese)

[3] Zhang PZ, Deng QD, Zhang ZQ, Li HB. Active faults, earthquake hazards and associated geodynamic processes in continental China. Scientia Sinica Terrae; **43**:1607-1620 (in Chinese)

[4] Kanamori H. 1977. The energy release in great earthquakes. Journal of Geophysical Research. 2013;**82**:2981-2987

[5] Stein S, Klosko E. Earthquake mechanisms and plate tectonics. International Geophysics. 2002;**81**(A):69-78. DOI: 10.1016/S0074-6142(02)80210-8

[6] Chen YT. Classification of earthquakes. City and Disaster. 2003;**1**:13-15 (in Chinese)

[7] Simms MJ. Uniquely extensive seismites from the latest Triassic of the United Kingdom: Evidence for bolide impact? Geology. 2003;**31**(6):557-560

[8] Wallace RE. Profiles and ages of young fault scarps, north-central Nevada. Geological Society of America Bulletin. 1977;**88**(9):1267-1278

[9] Yang ZE, Ying SH, Lin CY, Yu LB. Characteristics of fault rocks and their potential evidences for seismic events. Seismology and Geology. 1984;**3**(4):1-4 (in Chinese)

[10] Deng QD, Chen SF, Zhao XL. Tectonics, seismicity and dynamics of Longmenshan Mountains and its adjacent regions. Seismology and Geology. 1994;**16**(4):387-403 (in Chinese)

[11] Liu-Zeng J, Klinger Y, Xu X, Lasserre C, Chen G, Chen W, Tapponnier P, Zhang B. Millennial recurrence of large earthquakes on the Haiyuan fault near Songshan, Gansu Province, China. Bulletin of the Seismological Society of America. 2007;**97**(1B):14-34. DOI: 10.1785/0120050118

[12] McCalpin JP. Paleoseismology. San Diego: Academic Press; 2009. 647 p

[13] Ran YK, Li YB, Du P, Chen LC, Wand H. Key techniques and several cases analysis in paleoseismic studies in mainland China (3): Rupture characteristics, environment impact and paleoseismic indicators on normal faults. Seismology and Geology. 2014;**36**(2):287-301. DOI: 1.3969/j.issn.0253-4967.2014.02.001 (in Chinese with English abstract)

[14] Montenat C, Barrier P, d'Estevou PO, Hibsch C. Seismites: An attempt at critical analysis and classification. Sedimentary Geology. 2007;**196**:5-30

[15] Seilacher A. Fault-graded beds interpreted as seismites. Sedimentology. 1969;**13**:155-159

[16] Maltman A. On the term 'soft-sediment deformation. Journal of Structural Geology. 1984;**6**:589-592

[17] Brodzikowski K, van Loo AJ. A systematic classification of glacial and periglacial environments, facies and deposits. Earth-Science Reviews. 1987;**24**:297-381

[18] Qiao XF, Song TR, Gao LZ, Peng Y, Li HB, Gao M, Song B, Zhang QD. Seismic sequence in carbonate rocks by vibration liquefaction. Acta Geologica Sinica (English Edition). 1994;**7**(3):243-265

[19] Owen G, Moretti M, Alfaro P. Recognising triggers for soft-sediment deformation: Current understanding and future directions. Sedimentary Geology. 2011;**235**:133-140

[20] Qiao XF, Li HB, Qiu ZL. Seismites-paleoearthquake Records in Sedimentary Rock (the 10th paragraph). In: Feng ZZ. editor-in-chief. Beijing: Petroleum Industry Press; 2013. pp. 507-606 (in Chinese)

[21] He BZ, Qiao XF. Advances and overview on researching paleo-earthquake events: A review of seismites. Acta Geological Sinica. 2015;**89**(5):1702-1746

[22] Maltman AJ. Shear zones in argillaceous sediments—An experimental study. In: Jones ME, Preston RMF, editors. Deformation of Sediments and Sedimentary Rocks. Geological Society: London, Special Publication; 1987. 29 p

[23] Owen G. Deformation processes in Unconsolidated Sands. In: Jones ME, Preston RF. editor. Deformation of Sediments and Sedimentary Rocks. Geological Society of London Special Publication, 29. 1987. pp. 11-24

[24] Lowe DR. Water escape structures in coarse-grained sediments. Sedimentology. 1975; **22**:157-204

[25] Guiraud M, Plaziat JC. Seismites in the fluviatile bima sandstone: Identification of paleoseismism and discussion of their magnitudes in a cretaceous synsedimentary strike-slip basin (Upper Benue, Nigeria). Tectonophysics. 1993;**225**(4):493-522

[26] Allen JRL. Sedimentary Structures, their Character and Physical Basis, Vol. 2. Developments in Sedimentology. Vol. 30B. Amsterdam: Elsevier; 1982. 663 p

[27] Owen G, Moretti M. Identifying triggers for liquefaction-induced soft-sediment deformation in sands. Sedimentary Geology. 2011;**235**:141-147

[28] Van Loon AJ. Soft-sediment deformation structures in siliciclastic sediments: An overview. Geologos. 2009;**15**:3-55

[29] Du YS. Discussion about studies of earthquake event deposit in China. Journal of Palaeogeography. 2011;**13**(6):581-590 (in Chinese with English abstract)

[30] Obermeie SF. Use of liquefaction-induced features for paleoseismic analysis-an overview of how seismic liquefaction features can be distinguished from other features and how their regional distribution and properties of source sediment can be used to infer the location and strength of Holocene paleo-earthquakes. Engineering Geology. 1996;**44**:1-76

[31] Moretti M, Alfaro P, Caselles O, Canas JA. Modelling seismites with a digital shaking table. Tectonophysics. 1999;**304**:369-383

[32] Qiao XF, Song TR, Gao LZ, Li HB, Peng Y, Zhang CH, Zhang YX. Seismic Records in Strata (Ancient Earthquake). Beijing: Geological Publishing House; 2006. 1-263 p (in Chinese with English abstract)

[33] Van Loon AJ. The life cycle of seismite research. Geologos. 2014;**20**(2):61-66

[34] Ettensohn FR, Zhang C, Lierman R. Soft-sediment deformation in epicontinental carbonates as evidence of paleoseismicity with evidence for a possible new seismogenic indicator: Accordion folds. Sedimentary Geology. 2011;**235**:222-233

[35] Sims JD. Determining earthquake recurrence intervals from deformational structures in young lacustrine sediments. Tectonophysics. 1975;**29**:141-152

[36] Li HB, Fu XF, Van der Word J, Si JL, Wang ZX, Hou LW, Qiu ZL, Li N, Wu FY, Xu ZQ, Tapponnier P. Co-seisimic surface rupture and dextral-slip oblique thrusting of the Ms 8.0 Wenchuan earthquake. Acta Geologica Sinica. 2008;**82**(12):1623-1643 (in Chinese with English abstract)

[37] Li HB, Wang H, ZQ X, Si JL, Pei JL, Li TF, Huang Y, Song SR, Kuo LW, Sun ZM, Chevalie ML, Liu DL. Characteristics of the fault-related rocks, fault zones and the principal slip zone in the Wenchuan Earthquake Fault Scientific Drilling Project Hole—1 (WFSD-1). Tectonophysics. 2013;**584**:23-42

[38] Zhang PZ, We XZ, Shen ZK, Chen JH. Oblique high-angle listric-reverse faulting and associated straining processes: The Wenchuan earthquake of 12 May 2008, Sichuan, China. Annual Review of Earth and Planetary Sciences. 2010;**38**:353-382

[39] Fu BH, Shi PL, Wang P, Li Q, Kong P, Zheng GD. Geometry and kinematics of the Wenchuan earthquake surface ruptures around the Qushan Town of Beichuan County, Sichuan: Implications for mitigation of seismic and geologic disasters. Chinese Journal of Geophysics. 2009;**52**(2):485-495 (in Chinese with English abstract)

[40] Ran YK, Shi X, Wang H, Chen LC, Chen J, Liu RC, Gong H. The maximum coseismic vertical surface displacement and surface deformation pattern accompanying the Ms 8.0 Wenchuan earthquake. Chinese Science Bulletin. 2010;**55**(9):841-850

[41] Nichols RJ, Sparks RSJ, Wilson CJN. Experimental studies of the fluidization of layered sediments and the formation of fluid escape structures. Sedimentology. 1994;**41**:233-253

[42] Sobel ER, Arnaud N. Cretaceous-Paleogene basaltic rocks of the Tuyon basin, NW China and the Kyrgyz Tianshan: The trace of small plume. Lithos. 2000;**50**:191-215

[43] Li JH, Cai ZZ, Luo CS, Geng YH. The structure transfer at the southern end of Talas-Ferghana fault and its regional tectonic response in the Cenozoic. Acta Geologica Sinica. 2007;**81**(1):23-31 (in Chinese with English abstract)

[44] Luo JH, Zhou XY, Qiu B, Yang ZL, Yin H, Li JL. Controls of Talas-Ferghana fault on Kashi Sag. Northest Tarim Basin, Xinjiang. Petroleum Geology. 2004;**25**(6):584-587 (in Chinese with English abst)

[45] Owen G. Soft-sediment deformation in upper Proterozoic Torridonian sandstones (Applecross Formation) at Torridon, Northwest Scotland. Journal of Sedimentary Research. 1995;**A65**:495-504

[46] Liu Y, Xie JP. Vibration Liqueication of Sandy Soil. Beijing: Seismological press; 1984. pp. 1-327 (in Chinese with English abstract)

[47] Qiao XF, Jiang M, Li HB, et al. Soft-sediment deformation structures and their implications for tectonic evolution from Mesozoic to Cenozoic in the Longmen Shan. Earth Science Frontiers. 2016;**23**(6):80-106

[48] Li TD (Chief compiler). Geological Map of Western China and Adjacent Regions, 1:2500000. Beijing: Geologidal Pubulishing House. 2006

[49] Jia CZ, Wei GQ, Yao HJ. Oil and Gas Exploration Books in Tarim Basin- Tectonic Evolution and Regional Structural Geology. Beijing: Petroleum Industry Press; 1995; 70 p (in Chinese with English abstract)

[50] He DF, Jia CZ, Li DS, Zhang CJ, Meng QR, Shi X. Formation and evolution of polycyclic superimposed Tarim Basin. Oil & Gas Geology. 2005;**26**:64-77 (in Chinese with English abstract)

[51] Tang LJ, Jia CZ. Structure Interpretation and Stress Field Analysis in Superposition Tarim Basin/Series of Typical Superposition Basin Hydrocarbon Formation and Distribution Prediction in China. Beijing: Science Publishing House. 149 p; 2007 (in Chinese with English abstract)

[52] He BZ, Xu ZQ, Jiao CL, Li HB, Cai ZH. Tectonic unconformities and their formation: Implication for hydrocarbon accumulations in Tarim Basin. Acta Petrologica Sinica. 2011;**27**:253-265 (in Chinese with English abstract)

[53] He BZ, Jiao CL, Xu ZQ, Cai ZH, Zhang JX, Liu SL, Li HB, Chen WW, Yu ZY. The paleotectonic and paleogeography reconstructions of the Tarim Basin and its adjacent areas (NW China) during the late Early and Middle Paleozoic. Gondwana Research. 2016;**30**:191-206 http://dx.doi.org/10.1016/j.gr.2015.09.011

[54] He BZ, Qiao XF, Jiao CL, Xu ZQ, Cai ZH, Guo XP, Zhang YL. Palaeo-earthquake events during the late Early Palaeozoic in the central Tarim Basin (NW China): Evidence from deep drilling cores. Geologos. 2014;**20**(2):105-123. DOI: 10.2478/logos-2014-0006

[55] Rossetti DF, Bezerra FHR, Goes M, Neves BBB. Sediment deformation in Miocene and post-Miocene strata, Northeastern Brazil:Evidence for paleoseismicity in a passive margin. Sedimentary Geology. 2011;**235**:172-187

[56] Zhang HC. Thixotropic research of mud foundation triggered by earthquake. Journal of Geotechnical Engineering. 1989;**11**(3):78-85 (in Chinese)

[57] Tian HS, Zhang SH, Zhang AS. Test investigation on liquefied deformation structure in saturated lime-mud composites triggered by strong earthquakes. Acta Geological Sinica (English Edition). 2016;**90**(6):2008-2021

[58] Yang JS, Robinson PT, Jiang CF, Xu ZQ. Ophiolites of the Kunlun Mountains, China andtheir tectonic implications. Tectonophysics. 1996;**258**:215-231

[59] Xu ZQ, Yang JS, Li HB, Zhang JX, Wu CL. Orogenic Plateau: Terrain Amalgamation, Collision and Uplift in the Qinghai-Tibet Plateau. Beijing: Geological Publishing House; 2007. 458 pp (in Chinese with English abstract)

[60] Xu ZQ, Li ST, Zhang JX, Yang JS, He BZ, Li HB, Ling CS, Cai ZH. Paleo-Asian and Tethyan tectonic systems with docking the Tarim block. Acta Petrologica Sinica. 2011;**27**:1-22 (in Chinese with English abstract)

[61] Qiao XF, Gao LZ, Peng Y. Mesoproterozoic earthquake event and breakup of the Sino-Korean Plate. Acta Geologica Sinica (English Edition). 2007;**81**(3):385-397

[62] Song TR. A set of earthquake-tsunami sequences in carbonate stratigraphy of the Precambrian at thirteen imperial in Beijing. Sci. Rev. 1988;**38**(8):609-611 (in Chinese)

[63] Su DC, Qiao XF, Sun AP, Li HB, Somerville ID. Large earthquake-triggered liquefaction mounds and a carbonate sand volcano in the Mesoproterozoic Wumishan formation, Beijing, North China. Geological Journal. 2014;**49**:69-89

[64] Liu XY, Wang Q. Plate tectonic map of China's lithosphere. In: Ma LF, Qiao XF, Min LR, Fan BX, Ding XZ, editors. Geological Atlas of China. China: Geological Publishing House; 2007. pp. 41-44 (in Chinese)

[65] He ZJ, Song TR, Ding XZ, Zhang Q, Meng XH, Ge M. Early synsedimentary faulting of the Meso-Proterozoic Yanshan rift and its influence on event sedimentation. Journal of Palaeogeography. 2000;**2**:83-91 (in Chinese, with English abstract)

[66] Qiao XF, Gao LZ. Mesoproterozoic palaeoearthquake and palaeogeography in Yan-Liao Aulacogen. Journal of Palaeogeography. 2007;**9**:337-352 (in Chinese, with English abstract)

[67] Qiao XF. Intraplate seismic belt and basin framework of Sino-Korean plate in the Proterozoic. Earth Science Frontiers. 2002;**9**:141-150 (in Chinese, with English abstract)

[68] Su DC, Sun AP. Typical earthquake-induced soft-sediment deformation structures in the Mesoproterozoic Wumishan Fm., Yongding River valley (China) and interpreted earthquake frequency. Journal of Palaeogeography (English Edition). 2012;**1**:71-89

[69] Liu PJ. Seismite and its rhythm in the Gaoyuzhuang Formation of Mesoproterozoic in Pingquan County, Hebei Province. Geoscience. 2001;**15**:266-269 (in Chinese, with English Abstract)

[70] Liang DY, Song ZM, Zhao CH, Nie ZT. Discovery of Mesoproterozoic seismites at Baishi Mountain, Hebei Province and its geological significance. Geological Bulletin of China. 2002;**21**:625-630

[71] Liang DY, Nie ZT, Song ZM, Zhao CH, Chen KG, Gong HB. Seismic-tsunami sequence and its geological features of Mesoproterozoic Wumishan Formation in Fangshan Global Geopark, Beijing, China: A case study on Yesanpo scenic district. Geological Bulletin of China. 2009;**28**:30-37 (in Chinese, with English Abstract)

[72] Su WB, Zhang SH, Huff WD, Li HK, Ettensohn FR, Chen XY, Yang HM, Han YG, Song B, Santosh M. SHRIMP U-Pb ages of K-bentonite beds in the Xiamaling Formation: Implications for revised subdivision of the Meso- to Neoproterozoic history of the North China Craton. Gondwana Research. 2008;**14**:543-553

[73] Su WB, Li HK, Huff WD, Ettensohn FR, Zhang SH, Zhou HY, Wan YS. SHRIMP U-Pb dating for a K-bentonite bed in the Tieling Formation, North China. Chinese Science Bulletin. 2010;**55**:3312-3323

[74] Zhang CL, Wu ZJ, Gao LZ, Wang W, Tian YL, Ma C. Structure and significance of soft-sediment deformation structure of Wumishan formation triggered by earthquake. Science China Earth Sciences. 2007;**27**(3):336-342 (in Chinese with English abstract)

[75] Calvo JP, Rodriguez-Pascua M, Martin-Velazquez S, Jimenez S, Vicente GD. Micro-deformation of lacustrine laminite sequences from Late Miocene formations of SE Spain: An interpretation of loop bedding. Sedimentology. 1998;**5**(2):279-292

[76] Rodríguez-López JP, Meléndez N, Soria AR, Liesa CL, Van Loon AJ. Lateral variability of ancient seismites related to differences in sedimentary facies (the syn-rift Escucha formation, mid-cretaceous, eastern Spain). Sedimentary Geology. 2007;**201**:461-484

[77] Song TR, He ZJ, Ding XZ, Zhang QD. A study of geologidal event records in the proterozoic Chuanglinggou Formation of the Ming Tombs District, Beijing. Geological Review, 406. 2000;**46**(4):400 (in Chinese with English abstract)

[78] Su DC, Sun AP. Typical earthquake-induced soft-sediment deformation structures in the Mesoproterozoic Wumishan Formation, Yongding River Valley, Beijing, China and interpreted earthquake frequency. Journal of Palaeogeography. 2011;**1**(1):71-89

[79] Su DC, Sun AP. Soft-sediment deformation and occurrence frequency of palaeo-earthquake in the Mesoproterozoic Wumishan Formation, Yongding river valley, Beijing. Jourunal of Palaeogeography. 2011;**13**(6):591-614 (in Chinese with English abstract)

[80] He BZ, Qiao XF, Zhang YL, Tian HS, Cai ZH, Chen SQ, Zhang YX. Soft-sediment deformation structures in the Cretaceous Zhucheng depression, Shandong Province, East China; their character, deformation timing and tectonic implications. Journal of Asian Earth Sciences. 2015;**110**:101-122. DOI: 10.1016/j.jseaes.2014.12.005